Properties of MgO(100) ultrathin layers on Pd(100): Influence of the metal support

Livia Giordano,[1] Jacek Goniakowski,[2] and Gianfranco Pacchioni[1]
[1]*Dipartimento di Scienza dei Materiali, Università di Milano-Bicocca, Istituto Nazionale per la Fisica della Materia, Via Cozzi, 53, 20125 Milano, Italy*
[2]*Centre de Recherche sur les Mécanismes de la Croissance Cristalline, CNRS, Université de la Mediterranée, Campus de Luminy, 13288 Marseille, France*
(Received 24 September 2002; published 29 January 2003)

Using the full-potential linearized augmented plane wave (FP-LAPW) density functional approach we have studied the electronic and structural characteristics of free and palladium-supported MgO(100) thin films. For the unsupported MgO films we found a non-negligible reduction of the in-plane lattice parameters together with an expansion of the interlayer distances. The electronic structure is driven mainly by the thickness-induced gap reduction, compensated to a large extent by the gap opening due to the reduction of the interatomic distances. When a pseudomorphic MgO(100) monolayer is deposited on the Pd(100) surface, the palladium-oxygen interaction induces partially filled antibonding oxygen states at the Fermi level, showing a possible weak, substrate-induced, conductor behavior of the MgO layer, and resulting in a considerable reduction of its work function. Furthermore, we show that the properties of an oxygen vacancy in the supported MgO monolayer differ substantially from those of the perfect MgO(100) surface. In particular, one of the two electrons trapped in the vacancy is transferred to the metallic substrate. The characteristics of the perfect MgO(100) surface and of the corresponding oxygen vacancy are recovered for a two-layer film.

DOI: 10.1103/PhysRevB.67.045410 PACS number(s): 68.35.−p, 68.55.−a, 73.20.−r

I. INTRODUCTION

Ultrathin oxide films on metals and oxide-metal interfaces are of interest in many technological applications, ranging from microelectronics to catalysis and magnetic applications.[1–8] In recent years, thin oxide films grown on metals under ultrahigh-vacuum conditions have been widely used in surface science instead of single-crystal oxide substrates,[9] since they allow the use of techniques such as scanning tunneling microscopy, high-resolution energy loss, or photoelectron spectroscopies.[10–14] However, the thickness of the films traditionally used is of the order of 50–100 Å, and only very recently have ultrathin oxide films been studied as a class of materials that can display peculiar properties determined by the metal-oxide interface. Indeed, physical and chemical properties of ultrathin films of oxides, although expected to differ from those of their surfaces, are at present largely unknown. Additionally, the substrate generally modifies the atomic structure of the deposited ultrathin films (lattice parameters, rumpling and/or reconstructions). The structural constraints may have an additional effect on the electronic structure of the oxide film, which can be seen as an indirect effect of the substrate. On the other hand, the substrate may also modify the electronic structure of the deposited film directly by a chemical bonding and/or an interface charge transfer. Finally, nanometer-scale deposits can be stabilized in nonequilibrium structural states which may be preparation dependent. This increases the complexity of an experimental realization of this kind of system, but gives additional tools to modify its properties. An adequate choice of the substrate and of the deposition technique may thus be seen as a way of tuning the electronic and structural properties of the deposited film.

Ultrathin MgO(100) films on Ag(100) have been addressed both experimentally[15–23] and theoretically.[20,24,25] Ultraviolet photoelectron spectra have shown a moderate increase of the density of states at the Fermi level. This has been ascribed to antibonding oxygen states, and has been held responsible for an enhanced reactivity towards water.[18] On the other hand, theoretical calculations on MgO layers grown epitaxially on Ag(100)[24,25] do not seem to fit entirely this picture, and indicate only a very weak oxide-metal interaction, and thus a virtual absence of oxygen-silver bonding. Furthermore, a question of particular interest is the evolution of the respective metallic and insulating character under the mutual influence of the two components as a function of the growth mode and deposit coverage.[25]

To gain insight into the effect of the substrate on the properties of the deposited MgO thin film, we have considered a metallic substrate of different characteristics than silver. Palladium has a smaller lattice parameter, and thus a larger mismatch with respect to MgO (7%). This increases the effect of substrate-induced film deformation. Furthermore, the nature of the states at the Fermi level is different for the two metals: for Pd the Fermi level is positioned in the top part of the *d* band, while for Ag it is about 3 eV above the *d* band, and intersects the *sp* states. This results in a considerably lower density of states at the Fermi energy. We expect the substrate-induced modifications of the MgO thin film to be much more pronounced in the case of deposition on the Pd support. The comparison of the MgO/Pd interface with the well-characterized MgO/Ag interface can thus help to identify the importance of hybridization and charge-transfer mechanisms connected to the electronic structure of the metal substrate, compared to long-range polarization effects induced by the wide-gap oxide film. Finally, in order to separate the effect due to the metallic substrate we have also analyzed the effect of the layer thickness on the structural and electronic properties of unsupported MgO ultrathin (100) layers.

Experimentally, the growth of MgO thin films on Pd(100) surfaces has not been reported so far. One reason is that the technique usually adopted to grow MgO epitaxial films on metals, deposition of Mg in O_2 background pressure, leads to a partial oxidation of the Pd substrate. Our energetic results supply information on the possibility of a practical stabilization of the MgO thin-film deposits on the Pd(100) surface. On the other hand, on a more fundamental level, in the past many studies were devoted to Pd deposits on the MgO(100) surface,[26–28] whereas virtually no studies concerning the reverse situation (O/M) exist. Since, especially in the early growth stages, the properties of M/O and O/M are not necessarily symmetrical, we believe that such studies are important for a better understanding of the metal-oxide interface.

The paper is organized as follows. In Sec. II we describe the computational settings used for the present study. In Sec. III we present the results for unsupported MgO layers, while in Sec. IV the deposition-induced modifications of the MgO monolayer and bilayer are addressed. In Sec. V we focus on the characteristics of an oxygen vacancy in the supported MgO film.

II. TECHNIQUES

For the calculations we have used the density functional-based, full potential linear augmented plane-wave (FP-LAPW) method,[29] and the gradient-corrected form of the exchange-correlation potential by Perdew and Wang,[30] which was successfully applied to studies on surface processes and metal-oxide interfaces.[28,31] In particular, for a model of the Pd/MgO interface consisting of five layers of palladium on five layers of MgO, the calculated separation energy of 0.7 J/m^2 per interface unit cell correlates well with the experimental estimate of 0.75–0.9 J/m^2.[32] Conversely, analogous calculations with a local-density-approximation (LDA) exchange correlation potential[33] produce an adhesion energy of 1.6 J/m^2/interface unit cell. It should be noted, however, that recent results[34] have shown that in some cases LDA calculations give a better metal-oxide adhesion energy due to an accidental error cancellation in surface self-energy corrections. Within the FP-LAPW method, space is divided into nonoverlapping spheres centered on the atomic sites. Spheres of 1.8 a.u. radius were used for oxygen and magnesium atoms, and an 2.2 a.u. radius was used for palladium. The basis set consists of plane-wave envelope functions, augmented inside the atomic spheres by numerical solutions of the Schrödinger equation. We have used partial waves up to $l=10$ inside the atomic spheres, and have added the so-called ''local orbitals'' in order to include the $2s$ states of oxygen, $2s$ and $2p$ states of magnesium, and $4s$ and $4p$ states of palladium as semicore states. The plane-wave cutoff $K^2_{\max}$ was set equal to 20 Ry during the geometry optimization runs. Calculations with the cutoff increased to 28 Ry were performed for all the optimized geometries (except for unsupported MgO films, where $K^2_{\max}=20$ Ry gives already a good convergence) in order to estimate the separation energies, charge distributions, and densities of states. In particular, we have verified that the interface separation energy changes by less than 0.4% when increasing the cutoff parameter from 20 to 28 Ry. Additional results on the adequacy of this computational approach for representation of bulk Pd and MgO and of their surfaces, together with the results on the Pd/MgO(100) system can be found in Refs. 28 and 31.

In the present calculations the Pd surface was represented by a three-layer-thick, unrelaxed Pd slab with theoretical bulk Pd lattice parameter (3.97 Å). Calculations with a five-layer slab were performed for selected geometries to test the adequacy of our model. MgO was adsorbed symmetrically on both sides of the slab, and the vertical position of oxygen and magnesium atoms were optimized [(1×1) surface unit cell]. An isolated vacancy was approximated by a 0.25 vacancy coverage [(2×2) surface unit cell]. This corresponds to about a 6 Å distance between the vacancies, and has already proved to be a fairly adequate approximation.[28,35] In the vacancy calculations we have additionally taken into account the relaxation of the surface layer of the Pd substrate, and the horizontal displacements of the adsorbate atoms.

The k-point sampling of the Brillouin zone is converged to within 0.1 eV per atom (with a Gaussian broadening of 2 mRy). This is achieved with 15 k points in the irreducible part of the Brillouin zone. In order to compensate for the possible lack of full convergence with respect to computational settings, all calculations necessary for the determination of adsorption energies were performed with exactly the same periodic supercell.

III. UNSUPPORTED MgO(100) FILMS

In order to separate the effect of metal support on the properties of thin MgO layers we start our study by presenting the results on the structural and electronic characteristics of thin, unsupported MgO(100) layers. We consider MgO slabs of one, two, three, and four atomic layers. In all cases, while imposing the 1×1 periodicity, we have optimized the lattice parameters without any constraint on the interlayer spacing. The resulting formation energies (with respect to the bulk MgO cohesion energy), lattice parameters, and surface energies for MgO slabs of different thickness are summarized in Fig. 1 and Table I.

As expected, the lattice parameter and the formation energy decrease as function of the slab thickness, directly reflecting the increasing proportion of lower-coordinated (surface) atoms. These modifications are relatively well pronounced: both the reduction of the lattice parameters and of the formation energy between bulk MgO (sixfold-coordinated atoms) and a monolayer (fourfold coordinated atoms) are of the order of 8%. The reduction of in-plane lattice parameters $a_{//}$ induced by the surface stress is accompanied by a small (less than 2%) increase of the interlayer spacing $d_\perp$. We note that the overall convergence of the structural parameters and of the surface energy of MgO layers to the values of the perfect MgO(100) surface is relatively slow. On the other hand, by fixing the lattice parameters $a_{//}$ to the bulk value we find an extremely rapid convergence of the surface energy σ^*. Under this constraint, the modification of $d_\perp$ also remains smaller than 0.01 Å, thus approaching the characteristics of the perfect MgO(100) surface closely. These results clearly show the influence of the

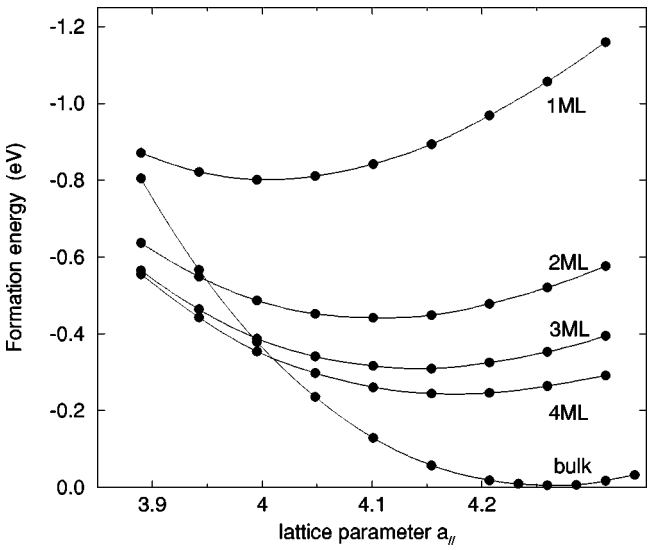

FIG. 1. Formation energy (eV/ MgO unit) computed with respect to the bulk MgO value (10.45 eV/ MgO unit) vs the lattice parameter (Å) for bulk MgO and for ultrathin MgO(100) films.

$a_{//}$ lattice parameter on the structural characteristics of the MgO layers, and the potential substrate-related flexibility.

It is worth noting that the reduction of the lattice parameter in the unsupported MgO films, and in the particular case of the 1-ML film, is not large enough to match neither the experimental (3.89 Å), nor the calculated (3.97 Å) lattice parameter of Pd. In all cases, an additional compression of MgO is necessary in order to match the two lattices at the interface. For a MgO monolayer, a 1% compression is sufficient to match the two lattices, and the related energy expense is 0.07 eV only. Both the compression and the energy expense increase rapidly with the slab thickness. We find about 0.40 eV, 0.78 eV, and 1.24 eV/interface units for two, three, and four MgO layers, respectively. In the limit of MgO and Pd at their bulk lattice parameters, one expects an 11 $\times$11 incommensurate interface structure, as reported in studies on Pd/MgO interfaces (see. e.g., Ref. 36, and references therein.)

The electronic characteristics of thin MgO(100) layers can be seen as resulting from two physical effects: (1) the slab thickness, and (2) the modification of the lattice parameter. In the following we will discuss the electronic structure of MgO slabs of different thickness at fixed (bulk) lattice parameter. Then for 1-ML MgO we will comment on the effect of the reduction of lattice parameter.

TABLE I. Calculated properties of unsupported MgO(100) thin films: in-plane lattice parameter $a_{//}$ (Å), interlayer spacing $d_{\perp}$ (Å) (for the 4-ML slab, 2.14 Å is the distance between the central layers), and surface energy σ (eV/surface MgO unit). σ^* (eV/surface MgO unit) corresponds to calculations with unrelaxed slabs (bulk MgO lattice parameter).

	Bulk	4 ML	3 ML	2 ML	1 ML
$a_{//}$	4.26	4.16	4.14	4.10	4.01
$d_{\perp}$	2.13	2.14, 2.16	2.17	2.18	-
σ	-	0.47	0.45	0.44	0.40
σ^*	-	0.52	0.52	0.52	0.53

TABLE II. Properties of unrelaxed MgO(100) thin layers: the change of the band gap, ΔE (eV), with respect to the bulk MgO value, and the change of the work function, $\Delta\phi$ (eV), with respect to the perfect surface (4-ML MgO).

	4 ML	3 ML	2 ML	1 ML	1 ML relaxed
ΔE	-1.3	-1.3	-1.4	-1.6	-1.3
$\Delta\phi$	-	0.1	0.1	0.0	0.1

Table II summarizes the main characteristics of the electronic structure of the unrelaxed MgO slabs: the change of the band gap with respect to the bulk MgO value, and of the work function ϕ (with respect to the 4-ML case, which we will use as the perfect surface reference). Although, as is well known, the absolute value of the electronic gap is not well reproduced in the ground-state density-funcitonal theory calculations, its evolution along the series reflects a physical effect. For MgO slabs with fixed lattice parameters we find a progressive reduction of the band gap as the slab thickness decreases. For the MgO monolayer, the reduction of the lattice parameter results in an increase of the gap, bringing its value back to that of a perfect surface (4-ML MgO). This evolution can be seen as a result of an overall weakening of the Madelung field when the slab thickness decreases (at the fixed lattice parameter). This induces an upward shift of the oxygen (anion) levels and a downward shift of the magnesium (cation) levels and results in a reduction of the band gap, as already discussed for MgO surfaces of different orientations.[4,37] Conversely, the reduction of the lattice parameter brings the ions closer to each other, reinforces the Madelung field, and thus has the opposite effect on the electronic structure. As a consequence, the modification of the electronic structure related to the change of the slab thickness is to a large extent compensated for by the reduction of the lattice parameter of the layer.[4,38]

The above interplay of electronic and geometric effects results in a modification of the potential seen by the molecules approaching the MgO surface. Without performing actual calculations of adsorption of a particular molecule, this modification can be estimated directly as a change of the electrostatic potential V_{elec} above the surface (here and in the following we will compare V_{elec} calculated at a fixed distance of 2.0 Å from the surface). Taking the rigid 4-ML slab as a perfect surface reference, in the case of a MgO monolayer, we find $\Delta V_{\mathrm{elec}}(\mathrm{O}) = -0.11$ (-0.06) eV, and $\Delta V_{\mathrm{elec}}(\mathrm{Mg}) = +0.17$ $(+0.06)$ eV, for the relaxed and fixed (values in the brackets) systems. Within the present sign convention (V_{elec} positive on top of oxygen and negative on top of magnesium), for the relaxed system, these modifications correspond to a 15% weakening of the electrostatic field above the surface.

IV. PD SUPPORTED MgO(100) MONOLAYER

In Sec. III we showed that the electronic properties of MgO slabs depend only weakly on the slab thickness and

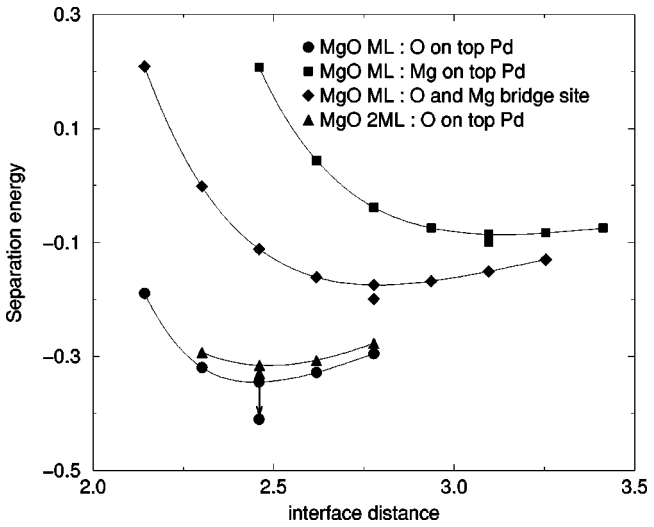

FIG. 2. Separation energy (eV) vs the interface distance (Å) calculated for 1-ML MgO deposited on the Pd(100) surface in three different geometries: O on top of Pd, Mg on top of Pd, O and Mg at the bridge positions, and for the 2-ML MgO deposited on top of the surface Pd. Arrows indicate the energy gain associated with the rumpling.

lattice parameters. In order to analyze the effect of the substrate we will describe the results obtained for pseudomorphic MgO(100) slabs deposited on the Pd(100) surface, focusing our attention on the monolayer and bilayer cases, respectively.

In order to determine the relative stability of different adsorption geometries we have calculated the separation energy $E_{\rm sep}$, defined as the difference between the total energy of the MgO/Pd(100) system, and those of the clean Pd slab and of the unsupported MgO film (at Pd lattice parameter). The results for the 1-ML MgO deposit are summarized in Fig. 2. The energetically most favorable adsorption site corresponds to oxygen atoms on top of Pd ($h_{\rm ads}=2.46$ Å, $E_{\rm sep}=0.35$ eV), while the less favorable structure corresponds to magnesium on top of Pd ($h_{\rm ads}=3.10$ Å, $E_{\rm sep}=0.09$ eV). The hollow surface site is intermediate ($h_{\rm ads}=2.78$ Å, $E_{\rm sep}=0.18$ eV). The above relative stability of different interface geometries also remains valid for thicker MgO films. Also the separation energies and the adsorption heights change little as a function of the MgO thickness. In particular, for the MgO bilayer in its preferential adsorption geometry (oxygen on top of Pd) we find $h_{\rm ads}=2.46$ Å and $E_{\rm sep}=0.31$ eV.

Contrary to the case of a free MgO monolayer, either at its equilibrium lattice parameters, or compressed to match the the Pd (100) lattice constant, the supported layer is not perfectly planar. When deposited (oxygen on top of Pd), the magnesium ions approach the Pd surface by about 0.16 Å more than the oxygen ions. The resulting rumpling of the MgO layer increases the separation energy by 0.07 eV. In the case of magnesium on top of Pd, the rumpling is 0.06 Å (the magnesium ions closer to the Pd surface) and the energy gain is less than 0.01 eV. In this latter case the rumpling is of the same order of magnitude as at the perfect MgO(100) surface (smaller than 0.05 Å). The relatively well-pronounced rumpling of the MgO monolayer in its preferential adsorption geometry is strongly smoothed by deposition of the second MgO layer.

The basic features of calculated adsorption geometry and energetics are very similar to those found for the deposition of MgO(100) layers on the Ag(100) surface.[24] In that case the separation energies are somewhat smaller, and the adsorption heights somewhat larger ($h_{ads}=2.6$ Å and $E_{sep}=0.3$ eV for oxygen on top of Ag, with rumpling). The present results fit well also with the general trends on metal/oxide interfaces as obtained for transition-metal monolayers deposited on the MgO(100) surface.[27] In particular, for Pd on the MgO(100) surface, the oxygen site is favored ($h_{\rm ads}=2.3$ Å, $E_{\rm sep}=0.5$ eV) over the magnesium one ($h_{\rm ads}=2.63$ Å, $E_{\rm sep}=0.2$ eV).[26] However, it is worth noting that in both cases, MgO/Pd and MgO/Ag,[24] the adsorption heights $h_{\rm ads}$ are systematically larger and the separation energies ($E_{\rm sep}$) systematically smaller compared to those of the corresponding metal/MgO systems, where a thin film of metal is deposited on the MgO(100) surface. This can be associated with the smaller horizontal lattice parameters of the MgO/metal interfaces (imposed by the substrate, rather than by the MgO) and, as a consequence, with weaker interaction in the direction perpendicular to the interface.

In order to determine the MgO growth mode on the Pd surface, the conventional approach consists of comparing the MgO(100) surface energy σ to the MgO/Pd(100) interface adhesion energy W. The cases $\sigma>W$ and $2\sigma<W$ correspond to the no-wetting and perfect wetting limits, respectively. If the calculated separation energy of 0.42 eV is used as a rough estimate of W, and the MgO surface energies from Table I are taken into account, $\sigma>W$, the theoretical prediction would correspond to a three-dimensional (3D) growth. However, the above method, valid for equilibrium micrometric deposits, does not take into account the atomic-scale effects and contributions, and may thus be not the best suited to discriminate between one-atomic-layer and somewhat thicker deposits. In the present case a direct comparison of calculated energies for monolayer and bilayer deposits may give a more adequate estimate. In fact, since the difference of energies between 1- and 2-ML films: $\left|\frac{1}{2}(E_{(2\text{ML MgO})/\text{Pd}}+E_{\text{Pd}})-E_{(1\text{ML MgO})/\text{Pd}}\right|$ is smaller than 0.05 eV/surface unit cell, within the accuracy of our calculations, we may expect an absence of a strong 3D growth tendency at the early MgO growth stages. In the following we present results on the electronic structure of the supported MgO monolayer, focusing on the preferential deposition geometry, namely, oxygen on top of Pd.

Figure 3 presents the DOS of the MgO/Pd(100) system, together with those of the clean Pd surface and the unsupported MgO layer. Energy scales of the panels are aligned so as to match the corresponding vacuum levels (zero of the potential far from the surface). The modifications due to the interface formation are mainly limited to the surface palladium layer (also confirmed by a test with a five-layer-thick Pd slab). The surface Pd band is broadened and its center of gravity is pushed toward lower energies with respect to the Fermi level. The formation of a weak chemical bond be-

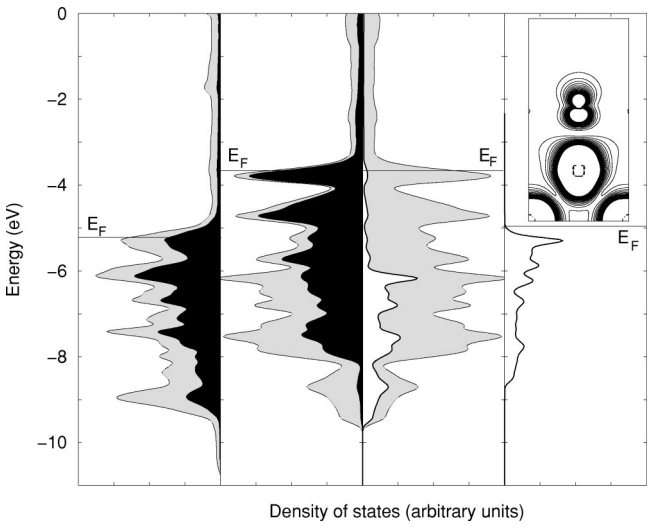

FIG. 3. DOS of the palladium (100) substrate (left-hand panel), of the MgO/Pd(100) system (two central panels), and of the unsupported MgO monolayer (right-hand panel). Total DOS's (gray) and projections on the surface palladium (black), and on MgO (white) are plotted. All DOS's are aligned at their respective vacuum level and convoluted by a 0.1 eV wide Gaussian function. In the inset, the contour plot of the electronic density at the Fermi level (± 0.3 eV) obtained for the MgO/Pd(100) system.

tween Pd and the MgO overlayer induces low-energy states at the bottom of the palladium density of states (DOS). The valence band of MgO is positioned 2 eV below the Fermi level. With respect to the unsupported MgO monolayer, its center of gravity is shifted downward. A hybridization between oxygen and palladium orbitals results in a strong deformation of the oxygen band, with the formation of a continuous spectrum of the metal-induced interface states in the gap of the MgO layer and, in particular, a peak of the oxygen local DOS (LDOS) at the Fermi level. The electronic density related to states in the vicinity of the Fermi level (± 0.3 eV) is displayed in the inset of Fig. 3. The net separation of the O_{sp} and Pd states shows the antibonding character of these Pd-O states. It is worth pointing out the similarity to the Pd-O bonding in the reversed system: Pd/MgO(100).[26]

With respect to MgO/Ag, where practically no oxygen states at the Fermi level have been found,[24,25] our results show that the *d* character of the palladium VBM and the stronger oxygen-metal hybridization result in a well pronounced presence of metal-induced gap states of oxygen character in the MgO's gap and in particular at the Fermi level.

We have performed an analysis of the charge transfer across the interface using a Bader-like method,[28,31,39] which consists of a partition of space into layers, delimited by the local minima of the electron density profile along the direction perpendicular to the interface. In the preferential adsorption geometry, we find that 0.14 electrons/interface unit cell are transferred from the MgO layer toward the surface palladium. This is consistent with the modification of the LDOS discussed above (namely, the partially empty oxygen AB states), or with the charge transfer found for the Pd/MgO(100) interface (0.10 electrons transferred from the MgO to the Pd deposit).[28] It is also coherent with the results on the MgO deposition on Ag(100) (Ref. 24), where a transfer of 0.2 electrons from oxygen to silver has been found.

Finally, the work function of the MgO/Pd system (3.65 eV) is considerably reduced with respect to the MgO (100) perfect surface (4.91 eV). This reduction is accompanied by a decrease of the Madelung potential above the surface (we find, respectively, $\Delta\ V_{\mathrm{elec}}(O) = -0.27$ eV and $\Delta\ V_{\mathrm{elec}}(\mathrm{Mg}) = +0.14$ eV with respect to the perfect MgO(100) surface). This effect may enhance the charge transfer between the MgO and the adsorbate, and modify its reactivity.

The LDOS of the pseudomorphic 2-ML MgO deposited on the Pd(100) surface shows that the substrate-induced modifications are principally limited to the interfacial layer. The MgO valence band (VB) of the oxygen atoms of the second layer are hardly modified and contribute little to the Fermi-level DOS. The rapid attenuation of the metal-induced characteristics with the increasing MgO slab thickness has already been pointed out for the MgO/Ag system.[25] With respect to the vacuum level, the valence-band maximum of the external MgO layer is positioned at 4.94 eV, thus close to its perfect surface value.

V. OXYGEN VACANCY IN THE SUPPORTED MgO(100) LAYER

Neutral surface oxygen vacancies, F_s^0 centers, are often held responsible for the surface reactivity. Their electronic structure at the perfect MgO(100) surface has already been thoroughly studied, and several consequences for the surface activity have been deduced. In particular, it has been shown that two electrons are trapped at the position of the missing oxygen atom, resulting in a doubly occupied gap state, localized about 2 eV above the MgO VB maximum.[35,40–43] Our calculations show that an oxygen vacancy in the surface layer of the deposited MgO bilayer recovers most of its perfect surface characteristics. The vacancy formation energies, which can be deduced from results on the Pd/MgO(100) and MgO(100) systems, show that the vacancies segregate to the interface (with respect to bulk MgO or to the perfect (100) surface).[28] Thus in the following we focus on the characteristics of an oxygen vacancy in a palladium-supported MgO monolayer (in its preferential adsorption geometry: oxygen on-top of palladium).

The formation energy for an isolated vacancy in a single palladium-supported MgO(100) layer is 7.2 eV, considerably smaller than that calculated for the perfect MgO(100) surface (9.5 eV), and estimated for the Pd/MgO(100) interface, 8.4 eV.[28] The lowering of the formation energy is a result of the stabilizing effect of the metal substrate, i.e., of the strong interaction of Pd with the oxygen vacancies at the MgO(100) surface, and of the low coordination of the vacancy in the MgO monolayer (cf. the decrease of cohesive energies as function of coordination). The average adsorption height of the oxygen deficient MgO layer, 2.3 Å, is smaller than for the perfect layer. The corrugation increases considerably (0.35 Å), mainly due to the Mg atoms surrounding the vacancy, which closely approach the substrate. These atoms

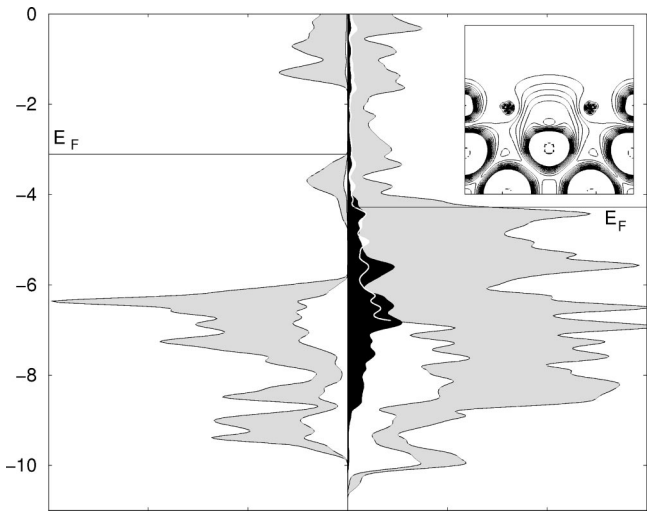

FIG. 4. Total and surface-projected DOS's for an oxygen vacancy on the perfect MgO(100) surface (left-hand panel), and in the palladium-supported MgO monolayer (right-hand panel). Total DOS (gray) and projections on the surface oxygens (white), and on the palladium atom underneath the vacancy (black) are plotted. DOS's are aligned at their respective vacuum level and convoluted by a 0.1 eV wide Gaussian function. In the inset, the contour plot of the electronic density at the Fermi level (-0.6 eV) is obtained for the oxygen vacancy in a palladium-supported MgO monolayer.

move also horizontally (by about 0.03 Å) outward from the vacancy, resulting in an overall shortening of the Mg-O distances. A similar structural effect has been found for the oxygen vacancy on the perfect MgO(100) surface, where, however, Mg atoms move somewhat upward.[35] The Pd atom directly under the missing oxygen is pulled out from the Pd surface by about 0.3 Å, to be compared with 0.5 Å in the Pd/MgO(100) case,[28] where a 2-ML Pd film was expanded horizontally in order to match the lattice parameters of the MgO substrate.

The presence of the oxygen vacancy and the related deformation of the MgO layer modify locally the electronic structure. In the following we compare the electronic characteristics of a vacancy in the palladium-supported MgO monolayer with those of a classic F_s^0 center on the perfect MgO(100) surface. Figure 4 presents the corresponding total and surface oxygen projected LDOS. The alignment of the energy scales is done by the respective vacuum levels. Fermi levels are plotted at the highest occupied state.

The main substrate-induced effect is the disappearance of the doubly occupied vacancy state, which at the perfect surface is placed at about 2 eV above the MgO VB maximum. This is a direct consequence of the strong hybridization between the vacancy state and the orbitals of the underlying palladium, and results in an electron transfer from the vacancy toward the substrate. In fact, a Bader-like analysis of the charge repartition reveals a 1.04 electron transfer from the MgO overlayer to the substrate. Although this estimation is necessarily approximate, if compared to the case of deposition of the defect-free MgO monolayer (where the electron transfer amounts to 0.14 only), we conclude that nearly one electron is transfered from the vacancy toward the underlying Pd substrate. As found by Sushko *et al.*[43] the vacancy state is higher in energy with respect to the typical Fermi energy of metal surfaces, (see Figs. 4 and 3, respectively) revealing the underlying microscopic mechanism of the observed charge transfer. In fact, electrons are transfered from the vacancy state to lower-lying Pd surface states until the related modification of potential at the interface aligns them on the energy scale, and stops further charge redistribution. As a consequence, we find the partially occupied vacancy state of the supported layer at the Fermi level (see the inset in Fig. 4). In the case of Pd(100) support, this results in a stabilization of a point defect which may be seen as the analogue of the surface F^+ center which, on the perfect MgO(100) surface, is much less stable than a neutral F_s^0 oxygen vacancy. However, it is important to stress that the electronic structures of the vacancy in the Pd supported MgO monolayer and in the ''classical'' F_s^+ center are substantially different. Contrary to the F_s^+ center, the oxygen vacancy in the supported MgO monolayer remains, at least within the local spin density approximation calculations, diamagnetic, and we thus expect a different response to adsorbates. Similar interface electronic structure, leading to an electron transfer from the vacancy to the metal, and resulting in a similarly charged state of the interfacial vacancy has already been found for the opposite configuration, namely Pd deposited on the oxygen deficient MgO(100) surface.[28] Our present study shows that this particular vacancy at the interface can be also stabilized in supported ultra-thin MgO layers, and exposed in this way to adsorbates. Since the properties of this kind of defects are strongly substrate-dependent, we propose a notation F_{Pd}^0 which, by taking the underlying metal, explicitly into account, can clearly distinguish them from classic, perfect surface F_s^0 centers.

In order to better illustrate the difference between the classic F_s^0 center and the F_{Pd}^0 defect, in Fig. 5 we plot maps of the electrostatic potential and electron density for the two defects. In both cases, the displayed plane contains the vacancy, the first neighbors Mg ions, and the third neighbors oxygen ions.

Electron density plots show very clearly the reduction of the electron population of the vacancy site. Additionally, they reveal the strong hybridization with the underlying palladium: in the case of supported MgO monolayer the electronic cloud loses the well-defined maximum and spatial expansion. As a consequence, the regions of positive electrostatic potential above the surface diminish. The relatively well pronounced repulsive contribution of the vacancy disappears totally, and it is the attractive potential of the neighboring cations which dominates the electrostatic interaction above the surface.

VI. CONCLUSIONS

Using a total-energy, density-functional approach, we have studied the electronic and structural characteristics of free and palladium-supported MgO(100) ultrathin films. We find that the structural parameters of the unsupported MgO(100) films vary significantly as a function of thickness, coupling the contraction of the in-plane lattice parameters to

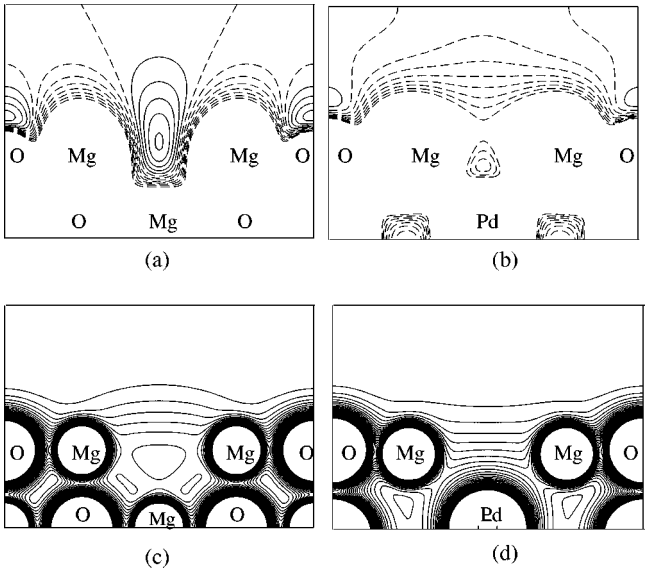

FIG. 5. Electrostatic potential (top row), and electron density (bottom row), of an oxygen vacancy at the perfect MgO(100) surface (left-hand column), and in the Pd supported MgO monolayer (right-hand column). Solid lines correspond to a positive potential (repulsive for electrons), and dashed lines represent a negative (attractive) potential.

an expansion of the interlayer distances. This structural deformation partially compensates for the effect due to low-coordinated atoms on the electronic structure. As a consequence, if fully relaxed, the electronic structure of MgO slabs is only weakly influenced by their thickness. If compared to a perfect MgO(100) surface, the differences are small, and one shall not expect any important change of the reactivity of MgO related to the film thickness.

For a pseudomorphic MgO deposit on the Pd(100) surface we have shown that its atomic structure and energetics (preferential adsorption site, adsorption height, and separation energy) reproduce the essential features of the Pd/MgO system and, more generally, fit the overall picture of the transition-metal/MgO interface well. Substrate-induced modifications of the electronic structure of MgO are determined principally by the hybridization between the metal and oxygen orbitals, and the formation of the metal induced gaps states in the band gap of deposited oxide. Since the extension of these states is limited to the interfacial MgO layer, the substrate-dependent modifications of the MgO reactivity are expected to be the strongest for the deposition of a single MgO layer, and related to the appearance of partially filled oxygen states at the Fermi level.

In general, the properties of the MgO/Pd(100) interface do not differ substantially from those of the MgO/Ag(100) system, despite the quite different band structure of the two metals. This is a result of the weak adhesion of the oxide film to the metal, which in turns reflects the modest importance of hybridization and charge-transfer contributions to the bonding, which are probably of comparable importance to the polarization induced by the ionic MgO layer on the metal electrons.[6]

One difference between Ag and Pd is the larger mismatch of the MgO/Pd interface and the resulting strain. The strain in MgO films supported on Ag(100) was analyzed in detail; it was shown that a complete release of strain is reached for a 9-ML film.[23] For MgO/Pd, we have shown that 1 ML of MgO is practically commensurate with Pd, while the strain will increase with films of a few ML thickness. In which way the strain will be removed remains unclear and the actual film morphology can be quite different from the ideal one, resulting in 3D island growth, as found for ultrathin MgO films on Ag(100).[22]

We find that an oxygen vacancy in the palladium-supported MgO(100) monolayer is stabilized by an important electron transfer from the vacancy toward the Pd substrate. As a consequence, its characteristics differ considerably from those of the classic neutral or charged F centers on the perfect MgO(100) surface. We propose a symbol F^0_{Pd} which reflects the influence of the underlying metal on the electronic structure of this kind of surface defect, and the related possibility of a fine tuning of their reactivity. In the case of a Pd substrate, our calculations show that surface F^0_{Pd} centers can be stabilized only in one-layer-thick MgO film.

ACKNOWLEDGMENTS

We thank C. Henry, G. Butti, M. Trioni, and N. Lopez for intersting and helpful discussions. The work of L.G. and G.P. was supported by the italian INFM through the PRA-ISADORA project and by MIUR through a PRIN project.

[1] *Metal-Ceramics Interfaces*, edited by M. Ruhle *et al.* (Pergamon, Oxford, 1990).
[2] G. A. Somorjai, *Introduction to Surface Chemistry and Catalysis* (Wiley, New York, 1994).
[3] V. E. Henrich and P. A. Cox, *The Surface Science of Metal Oxides* (Cambridge University Press, Cambridge, 1994).
[4] C. Noguera, *Physics and Chemistry at Oxide Surfaces* (Cambridge University Press, Cambridge, 1995).
[5] G. Bordier and C. Noguera, Phys. Rev. B **44**, 6361 (1991).
[6] F. Didier and J. Jupille, Surf. Sci. **314**, 378 (1994).
[7] M. W. Finnis, J. Phys.: Condens. Matter **8**, 5811 (1996).
[8] S. A. Chambers, Surf. Sci. Rep. **39**, (2000).
[9] H. J. Freund, H. Kuhlenbeck, and V. Staemmler, Rep. Prog. Phys. **59**, 283 (1996).
[10] D. W. Goodman, J. Vac. Sci. Technol. A **14**, 1526 (1996).
[11] T. Bertrams and H. Neddermeyer, J. Vac. Sci. Technol. B **14**, 1141 (1996).
[12] C. A. Ventrice, T. Bertrams, H. Hannemann, A. Brodde, and H. Neddermeyer, Phys. Rev. B **49**, 5773 (1994).
[13] *Chemisorption and Reactivity on Supported Clusters and Thin Films*, Vol. 331 of NATO Advanced Study Institute, Series E: Science, edited by R. M. Lambert and G. Pacchioni (Kluwer, Dordrecht, 1997).
[14] G. Renaud, Surf. Sci. Rep. **32**, 1 (1998).

[15] J. Wollschläger, D. Erdös, and K. M. Schröder, Surf. Sci. **402/404**, 272 (1998).
[16] J. Wollschläger, J. Viernow, C. Tegenkamp, D. Erdös, K. M. Schröder, and H. Pfnür, Appl. Surf. Sci. **142**, 129 (1999).
[17] S. Altieri, L. H. Tjeng, F. C. Voogt, T. Hibma, and G. A. Sawatzky, Phys. Rev. B **59**, R2517 (1999).
[18] S. Altieri, L. H. Tjeng, and G. A. Sawatzky, Phys. Rev. B **61**, 16 948 (2000).
[19] S. Valeri, S. Altieri, A. di Bona, C. Giovanardi, and T. S. Moia, Thin Solid Films **400**, 16 (2001).
[20] C. Giovanardi, A. di Bona, T. S. Moia, S. Valeri, C. Pisani, M. Sgroi, and M. Busso, Surf. Sci. **505**, L209 (2002).
[21] M. Kiguchi, T. Goto, K. Saiki, T. Sasaki, Y. Iwasawa, and A. Koma, Surf. Sci. **512**, 97 (2002).
[22] S. Valeri, S. Altieri, U. del Pennino, A. di Bona, P. Luches, and A. Rota, Phys. Rev. B **65**, 245410 (2002).
[23] S. Valeri, S. Altieri, A. di Bona, P. Luches, C. Giovanardi, and T. S. Moia, Surf. Sci. **507-510**, 311 (2002).
[24] M. Sgroi, C. Pisani, and M. Musso, Thin Solid Films **400**, 64 (2001).
[25] S. Schintke, S. Messerli, M. Pivetta, F. Patthey, L. Libioulle, M. Stengel, A. De Vita, and W. -D. Schneider, Phys. Rev. Lett. **87**, 276801 (2001).
[26] J. Goniakowski, Phys. Rev. B **57**, 1935 (1998).
[27] J. Goniakowski, Phys. Rev. B **59**, 11 047 (1999).
[28] L. Giordano, J. Goniakowski, and G. Pacchioni, Phys. Rev. B **64**, 075417 (2001).
[29] P. Blaha, K. Schwarz, and J. Luitz, WIEN97, Vienna University of Technology 1997. [Improved and updated Unix version of the original copyrighted WIEN-code, which was published by P. Blaha, K. Schwarz, P. Sorantin, and S. B. Trickey, in Comput. Phys. Commun. **59**, 399 (1990)].
[30] J. P. Perdew, K. Burke, and Y. Wang, Phys. Rev. B **54**, 16 533 (1996).
[31] J. Goniakowski, and C. Noguera, Phys. Rev. B **60**, 16 120 (1999); **66**, 085417 (2002).
[32] H. Graoui, S. Giorgio, and C.R. Henry, Philos. Mag. B **81**, 1649 (2001).
[33] J.P. Perdew and Y. Wang, Phys. Rev. B **45**, 13 244 (1992).
[34] A. E. Mattsson and D. R. Jennison, Surf. Sci. **520**, L611 (2002).
[35] F. Finocchi, J. Goniakowski, and C. Noguera, Phys. Rev. B **59**, 5178 (1999).
[36] W. Vervisch, C. Mottet, J. Goniakowski, Phys. Rev. B **65**, 245411 (2002).
[37] J. Goniakowski and C. Noguera, Surf. Sci. **319**, 68 (1994); **319**, 81 (1994).
[38] J. Goniakowski and C. Noguera, Surf. Sci. **323**, 129 (1995); **340**, 191 (1995).
[39] R. F. W. Bader, Chem. Rev. **91**, 983 (1991).
[40] A. M. Ferrari and G. Pacchioni, J. Phys. Chem. **100**, 9032 (1996).
[41] L. N. Kantorovich, J. M. Holender, and M. J. Gillan, Surf. Sci. **343**, 221 (1995).
[42] E. Scorza, U. Birkenheuer, and C. Pisani, J. Phys. Chem. **107**, 9645 (1997).
[43] P. V. Sushko, A. L. Shluger, and C. R. A. Catlow, Surf. Sci. **450**, 153 (2000).